

Peierls-Hubbard Finite Systems: A General Method

Roberto E. Lagos

Departamento de Física • IGCE Universidade Estadual Paulista • UNESP
Caixa Postal 178, 13500-230 Rro Claro, SP, Brasil

Received November 11, 1992

We extend a continued matrix method, developed earlier, to solve finite size Peierls-Hubbard Hamiltonians. In particular, we solve the dimer case, compare with existing results, and discuss the advantages of the method presented: it can be generalized, in a straightforward and systematic fashion, to larger systems; the method is amenable to the introduction of small "fields", necessary to break symmetries in finite systems, therefore enabling us to probe the stability of the various ordered states; furthermore it allows the computation of observables in a simple and economic fashion; and the several approximations available for infinite systems can be tested and compared as function of the system's size.

I. Introduction

Peierls-Hubbard Hamiltonians (PHH) consider the interplay of electron-electron and electron-lattice interactions, of relevance in a large variety of problems in both condensed matter and molecular physics, e.g., charge transfer, metal-insulator transitions, valence fluctuations, bond order and so on. As examples we mention: numerical^[1-4], variational^[5] and mean field^[6] approaches to one and two dimensional PHH, all within the adiabatic approximation^[7]; and a non-adiabatic effective medium approach^[8]. Also perturbative methods have been utilized, as in refs. [9, 10] to deal with organic ion-radical compounds and probe their microscopic parameters via optical lineshape calculations. General solutions for finite PHH are desirable not only to study energy transport and lineshapes of molecular clusters, they also provide guidelines to probe the validity of existing approximations for infinite systems, as the system size is increased. We developed a Green's Function Matrix Continued Fraction Method for exciton-phonon interacting systems^[11-14], and apply it here to PHH (see also refs. [15-17] for related methods).

II. Peierls-Hubbard Hamiltonian

A cluster with N sites, N electrons and N_m lattice modes is modeled with the Hamiltonian

$$\mathbf{H} = \mathbf{H}_{\text{el}} + \mathbf{H}_{\text{ph}} + \mathbf{H}_{\text{ep}}, \quad (1)$$

with

$$\mathbf{H}_{\text{el}} = \sum T_{ij} c_i^\dagger c_j + \sum U_{ijkl} c_i^\dagger c_j^\dagger c_k c_l,$$

$$\mathbf{H}_{\text{ph}} = \sum \omega_\alpha b_\alpha^\dagger b_\alpha,$$

$$\mathbf{H}_{\text{ep}} = \sum \mathcal{M}_\alpha^{ij} c_i^\dagger c_j (b_\alpha^\dagger + b_\alpha),$$

where \mathbf{H}_{el} is the electronic, \mathbf{H}_{ph} the lattice, and \mathbf{H}_{ep} the electron-lattice contribution to \mathbf{H} , respectively; i a site (and spin) index ($i \leq N$), α a lattice mode index ($\alpha \leq N_m$). The T 's and U 's are transfer and Coulomb repulsion terms respectively. The ω 's are the several lattice modes (in the harmonic approximation) and the \mathcal{M} 's the (linear) electron-lattice interaction strength. The operator c (b) destroys an electron (phonon) at site i , spin σ (mode α). Since the total number of electrons N is a constant of the motion, the Hamiltonian can be reduced to a similar Hamiltonian $\mathbf{H}_{\mathbf{r}}$ with renormalized ($T, U, \omega, \mathcal{M}$)'s with $N_m - 1$ modes plus a decoupled displaced oscillator (mode B , frequency Ω and strength λ), namely as:

$$\mathbf{H} = \mathbf{H}_{\mathbf{r}} + \Omega B^\dagger B + \lambda(B^\dagger + B). \quad (2)$$

Now and throughout, our \mathbf{H} will stand for the reduced $\mathbf{H}_{\mathbf{r}}$; solutions of the full Hamiltonian (1) are necessary, for example, to compute the actual optical lineshapes^[18].

Here we present the zero temperature, one mode ($N_m - 1 = 1$) case. For the general case approximations have been developed^[12-14,19]. The exact solution is obtained in several steps, as sketched below (see details in [11,12]):

i) Solve for \mathbf{H}_{el} and obtain a basis set $|\phi_j\rangle$, $j \leq N_s$, with N_s the number of electronic states, in general greater than N .

ii) Calculate the electron-phonon interacting matrix \mathbf{M} with components

$$\mathbf{M}_{ij} = \langle \phi_i | \sum_{kl} \mathcal{M}_{kl} c_k^\dagger c_l | \phi_j \rangle$$

iii) Define the (retarded) Green's Function Matrix $\mathbf{G}(z)$ with components

$$\mathbf{G}_{ij}(z) = -i \int_0^{\infty} dt e^{izt} \langle\langle |\phi_i(t)\rangle \langle\phi_j(0)| \rangle\rangle, \quad (3)$$

with $\text{Im}z = \epsilon^+$, ($\langle\langle \dots \rangle\rangle$) denotes average over both the electron and phonon vacuum and the time evolution of $|\phi_i(t)\rangle$ is given by \mathbf{H}_R . If the full solution is needed, \mathbf{G} must be replaced by \mathcal{G} , a Poissonian convolution of \mathbf{G} with the displaced decoupled oscillator^[20], given by

$$\mathcal{G}(z) = e^{-g} \sum_{l=0}^{\infty} \frac{g^l \mathbf{G}[z - (g-l)\Omega]}{l!}, \quad (4)$$

with $g = (\lambda/\Omega)^2$, see equation (2).

iv) Define the pure electronic Green's Function $\mathbf{G}_0(z)$, as in iii) but with the time evolution of $|\phi(t)\rangle$ given by \mathbf{H}_{e1} .

v) Define an auxiliary function $\mathbf{D}(z)$ satisfying a Dyson Type equation, see for example^[11-14]

$$\mathbf{D}(z) = \mathbf{G}_0(z) + \mathbf{G}_0(z)\mathbf{H}_{ep}\mathbf{D}(z). \quad (5)$$

$\mathbf{D}(z)$ has matrix components, $\langle n|\mathbf{D}(z)|m\rangle$, on the electronic Hilbert space ($i, j \leq N$) and on the harmonic oscillator Hilbert space ($|n\rangle, |m\rangle; n, m = 1, 2, \dots$). Throughout this paper, we keep matrix notation for the electronic part and display explicitly the oscillator's components.

Finally, the solution is $\mathbf{G}(z) = \langle 0|\mathbf{D}(z)|0\rangle$, with the recursion relations (see again, refs. [11-14])

$$\langle m|\mathbf{D}(z)|n\rangle = \mathbf{G}_0(z)\delta_{mn} + \mathbf{G}_0(z)\mathbf{M}\langle m|\Theta(z)|n\rangle, \quad (6)$$

where

$$\Theta(z) = b^\dagger \mathbf{D}(z + \omega) + b \mathbf{D}(z - \omega).$$

The diagonal part can be solved via a continued matrix algorithm as

$$\langle n|\mathbf{D}(z)|n\rangle^{-1} = \mathbf{G}_0^{-1}(z) - \theta_n(z), \quad (7)$$

with

$$\theta_n(z) = \mathbf{M} \frac{n+1}{\mathbf{G}_0^{-1}(z - \omega) - \theta_{n+1}(z - \omega)} \mathbf{M},$$

and $n > 0$. Now, for N_m modes with frequency ω , and interaction matrix \mathbf{M}_α , with $1 \leq \alpha \leq N_m$, a sound approximation^[13,14,19] was found to be

$$\theta_n(z) = \sum_{\alpha=1}^{N_m} \mathbf{M}_\alpha \frac{n+1}{\mathbf{G}_0^{-1}(z - \omega_\alpha) - \theta_{n+1}(z - \omega_\alpha)} \mathbf{M}_\alpha.$$

The information contained in $\mathbf{G}(z)$ is extracted via expectation values and susceptibilities probing our system with small external fields. Any given operator \mathbf{A}

may be decomposed as $\mathbf{A} = \mathbf{A}_e \mathbf{A}_p$ where \mathbf{A}_e is the electronic, and \mathbf{A}_p the lattice part of \mathbf{A} , respectively. Let's define the spectral density of such operator as

$$\mathbf{S}_\mathbf{A}(z) = -\frac{\text{Im}}{\pi} \sum_n \text{Trace} \mathbf{A}_e \langle 0|\mathbf{D}(z)|n\rangle \langle n|\mathbf{A}_p|0\rangle. \quad (8)$$

If a small external static field \mathcal{H} is introduced, by adding to \mathbf{H} the incremental $\Delta\mathbf{H} = -0.5\mathcal{H}\mathbf{B}$, with \mathbf{B} the conjugate operator to \mathbf{H} , and with $n(z)$ the spectral density of the identity operator (the density of states DOS), then the expectation value ($\langle\langle \mathbf{A}(z) \rangle\rangle$) and the susceptibility $\chi_\mathbf{B}(z)$ can be cast, respectively as

$$\begin{aligned} \langle\langle \mathbf{A}(z) \rangle\rangle &= \frac{\mathbf{S}_\mathbf{A}(z)}{n(z)} \\ \chi_\mathbf{B}(z) &= \lim_{\mathcal{H} \rightarrow 0} \frac{\langle\langle \mathbf{B}(z) \rangle\rangle}{\mathcal{H}} \end{aligned} \quad (9)$$

To solve for $\mathbf{G}(z)$ is equivalent to find the normalized eigenvectors and eigenvalues $|\psi_\mu\rangle, \varepsilon_\mu$ of \mathbf{H} , respectively. This equivalence may be displayed as

$$\langle\langle \mathbf{A}(\varepsilon_\mu) \rangle\rangle = \langle \psi_\mu | \mathbf{A} | \psi_\mu \rangle.$$

III. The Dimer Case

Consider a two site, two electron system ($N = 2$, the smallest finite size counterpart to the half filled band case), with diagonal electron-lattice interaction $\mathcal{M}_{ii} = S^{1/2}$ and off-diagonal electron-lattice interaction $\mathcal{M}_{12} = \kappa$. Periodic boundary conditions require us to take both sites and modes to be identical, a restriction to be lifted without further complications, if we want to study for example, a heteronuclear diatomic molecule. From the two normal modes (frequency ω), conveniently written as

$$b_\pm = \sqrt{1/2}(b_1 \pm b_2),$$

the symmetric mode (+) is decoupled when reducing the Hamiltonian, as in equation (2), with $\mathbf{B} = b_+$. Also the only relevant Coulomb term is the intrasite repulsion U (all others' eliminated via the constant of the motion N into effective T and U). Also we introduce a staggered "electric" and "magnetic" field; h_q and h_s , respectively, in order to study charge and spin transfer states, precursor states for charge and spin density waves in infinite systems. These fields are essential in finite systems, as symmetry breaking devices.

Then, the reduced Hamiltonian \mathbf{H} is

$$\mathbf{H} = \mathbf{H}_{e1} + \mathbf{H}', \quad (10)$$

with

$$\mathbf{H}_{e1} = -0.5(h_q Q + h_s m_\sigma) - TB + U \sum_\sigma n_{i\uparrow} n_{i\downarrow}, \quad (11)$$

and

$$\mathbf{H}' = \omega b_-^\dagger b_- + [\sqrt{S/2}Q + \kappa\mathcal{B}](b_-^\dagger + b_-), \quad (12)$$

with

$$\begin{aligned} \mathcal{B} &= \sum_{\sigma} (c_{1\sigma}^\dagger c_{2\sigma} + c_{2\sigma}^\dagger c_{1\sigma}), \\ Q &= \sum_{\sigma} (n_{1\sigma} - n_{2\sigma}), \\ m_{\sigma} &= \sum_{\sigma} \sigma (n_{1\sigma} - n_{2\sigma}), \end{aligned}$$

which represent the bond strength, charge transfer and spin transfer operators, respectively. The electronic basis set is $|\phi_i\rangle$, $i = 1 - 4$, with

$$|\phi_{1,2}\rangle = \sqrt{1/2}(c_{1\uparrow}^\dagger c_{2\downarrow}^\dagger \pm c_{1\downarrow}^\dagger c_{2\uparrow}^\dagger) |0\rangle,$$

and

$$|\phi_{3,4}\rangle = \sqrt{1/2}(c_{1\uparrow}^\dagger c_{1\downarrow}^\dagger \pm c_{2\uparrow}^\dagger c_{2\downarrow}^\dagger) |0\rangle,$$

where $|0\rangle$ is the electronic vacuum. The two remaining triplet states have no matrix elements in the relevant Hilbert space. Then, the electronic Green's function \mathbf{G}_0 is given by

$$\mathbf{G}_0^{-1}(z) = \begin{pmatrix} z & h_{\sigma} & 0 & 0 \\ h_{\sigma} & z & 0 & 2T \\ 0 & 0 & z - U & h_q \\ 0 & 2T & h_q & z - U \end{pmatrix}. \quad (13)$$

Let us define the following auxiliary matrix

$$\mathbf{\Gamma}(a, b, c) = \begin{pmatrix} 0 & a & 0 & 0 \\ a & 0 & 0 & b \\ 0 & 0 & 0 & c \\ 0 & b & c & 0 \end{pmatrix}. \quad (14)$$

Then, in the electronic basis, the bond strength, charge transfer and spin transfer operators defined above are represented by

$$\mathbf{A}_{\mathcal{B}} = \mathbf{\Gamma}(0, 2, 0), \quad \mathbf{A}_Q = \mathbf{\Gamma}(0, 0, 2), \quad \mathbf{A}_{\sigma} = \mathbf{\Gamma}(2, 0, 0),$$

respectively, and the interacting matrix \mathbf{M} is given by $\mathbf{M} = \sqrt{2S}\mathbf{A}_Q + \kappa\mathbf{A}_{\mathcal{B}}$.

IV. Results

The dimer, for the diagonal case ($t_i = 0$), has been solved in the adiabatic limit^[21] and via direct

diagonalization^[22-25] (ref. [26] considers the off-diagonal phonon). In all these cases no spin susceptibility was calculated, so the relevant basis set required only the three singlet states $|\phi_i\rangle$, $i = 2, 3, 4$. We need to increment the basis set in order to include the triplet state with the z spin component equal to zero ($i=1$); thus we notice the first advantage of the method presented here: with a single stroke we incorporate both charge (with or without lattice deformation) and spin symmetry breaking devices, introducing the "small" fields. Our formalism allow us to classify in a natural fashion any state, say with energy ε_0 , as being either a spin transfer (STS) or a charge transfer (QTS) state. We do this by computing both the spin and charge transfer susceptibilities, at equal strength fields. The STS is probed with the condition

$$\rho = \left| \frac{\chi_{\sigma}(\varepsilon_0)}{\chi_Q(\varepsilon_0)} \right| > 1. \quad (15)$$

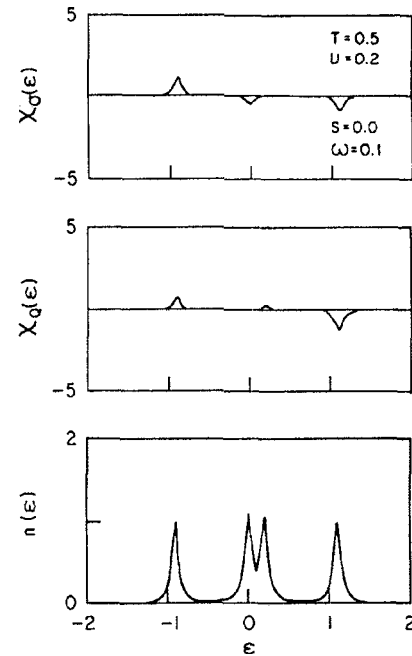


Figure 1: $n(\varepsilon)\chi_Q(\varepsilon)$ and $\chi_{\sigma}(\varepsilon)$, for the parameter set $T = 0.5$, $U = 0.2$, $S = 0.0$ and $\omega = 0.1$.

Conversely the QTS is probed requiring $\rho < 1$. The lattice deformation is quantified with the bond strength ratio

$$\xi = \left| \frac{\langle\langle \mathcal{B}(\varepsilon_0) \rangle\rangle}{\langle\langle \mathcal{B}_0(\varepsilon_0) \rangle\rangle} \right|, \quad (16)$$

where the subscript 0 in \mathcal{B} means the expectation value is evaluated at the null value for the lattice parameters ($S = \kappa = w = 0$). The sign of ρ , if no absolute value was taken merely defines the parity of the state. For a given set of parameters (T, U, S, κ, w) the character of

the system is defined according to the character of the ground state. Any given state shows as a simple pole of the DOS $n(\epsilon)$. For computational and display purposes we use a finite energy imaginary part δ , therefore poles will be displayed as local maxima. A qualitative classification for the STS or QTS character of the system^[21,23,24], for the diagonal case ($\kappa = 0$ and hereafter restrict to this case) is: the former occurs in the small S/T , large U/T regions of parameter space and the latter (possibly accompanied by a lattice distortion) for large S/T , small U/T or small ω/T . Therefore U (Coulomb correlations) and S (electron lattice interactions) compete to define the STS or QTS character of the system. Particular cases are (for infinite systems) the insulating antiferromagnet ($U \gg T, S \ll U$) and the Peierls Instability ("band limit" with $S, T \gg U$). We plot the DOS and both susceptibilities, as function of energy with an energy imaginary part $\delta = 0.05$ and fields $h_Q = h, \approx 10^{-7}$ in dimensionless units. In Figures 1 and 2 we consider the pure electronic case (i.e. $S = 0$) for two sets of values for T and U . In both cases the system has a STS character, the transition to QTS only to occur exactly at $U = 0$ refs. [21, 23, 24]. As S is increased (say for fixed U) there is a smooth crossover to QTS, in agreement with^[23-25]. In Figures 3 and 4, for the same values of T and U , but with $S = 0.5$, a clear QTS regime is displayed. Notice that excited states in both cases are STS, the effect more pronounced for the case $U > T$. Furthermore Figures 5 and 6 with $S = 1.0$ show the same trends as is the previous set of Figures, also highlighting the vast number of excited states and their symmetries (parity) on both their spin and charge attributes (given by the sign of the susceptibilities at the poles). The boundary between STS and QTS can be calculated in parameter space. Let us remark that our spectral densities are, due to the finite size of our system, of the type

$$S_{\mathbf{A}}(z) := \sum_{\mu=0}^{\infty} n(\epsilon_{\mu}) \langle \psi_{\mu} | \mathbf{A} | \psi_{\mu} \rangle \delta(z - \epsilon_{\mu}),$$

where the μ is the eigenvalue index and ψ_{μ} the normalized eigenvector as defined at the end of section II. Therefore the spectral densities will be very sensitive to the actual value of the energy's imaginary part δ , both on the computed values for the poles (eigenvalues) and for the residues (expectation values) as well. Thus, caution must be exercised as a "small" δ is chosen. Fortunately, this numerical inconvenience is easily surmounted with a fast analytic continuation algorithm as in ref. [27]. In fact, only in order to determine the ground state energy such caution should apply, all other observables are ratios of spectral densities, the latter found to be weakly dependent on the smallness of δ . Notice that all matrix elements of $\mathbf{G}(z)$ are determined in one stroke and that the diverse observables are ob-

tained as the imaginary part of linear combinations of the $\mathbf{G}(z)$'s matrix elements.

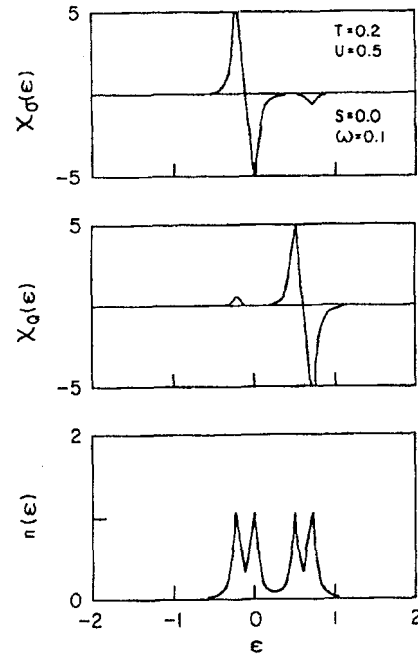


Figure 2: $n(\epsilon), \chi_Q(\epsilon)$ and $\chi_S(\epsilon)$, for the parameter set $T = 0.2, U = 0.5, S = 0.0$ and $\omega = 0.1$,

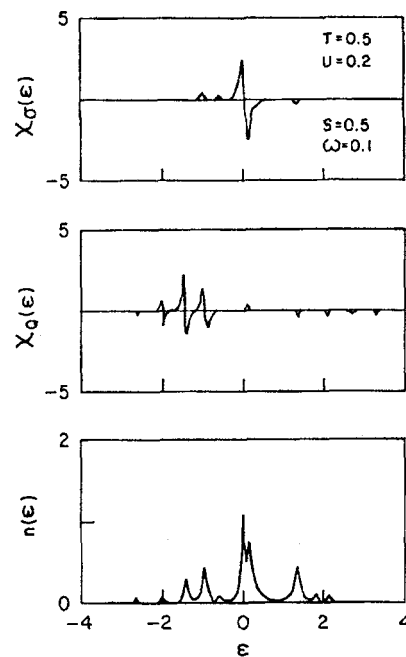


Figure 3: $n(\epsilon), \chi_Q(\epsilon), \chi_S(\epsilon)$ (see text), for the parameter set $T = 0.5, U = 0.2, S = 0.5$ and $\omega = 0.1$.

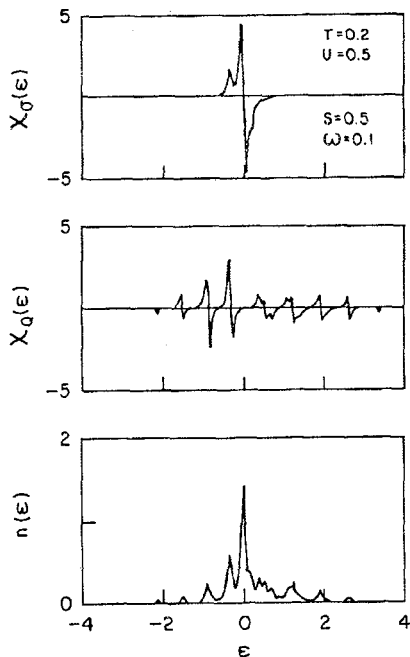


Figure 4: $n(\epsilon)$, $\chi_Q(\epsilon)$ and $\chi_\sigma(\epsilon)$, for the parameter set $T = 0.2$, $U = 0.5$, $S = 0.5$ and $w = 0.1$.

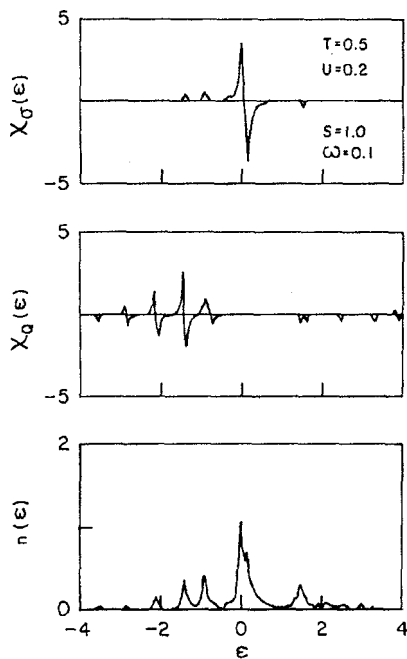


Figure 5: $n(\epsilon)$, $\chi_Q(\epsilon)$ and $\chi_\sigma(\epsilon)$, for the parameter set $T = 0.5$, $U = 0.2$, $S = 1.0$ and $w = 0.1$.

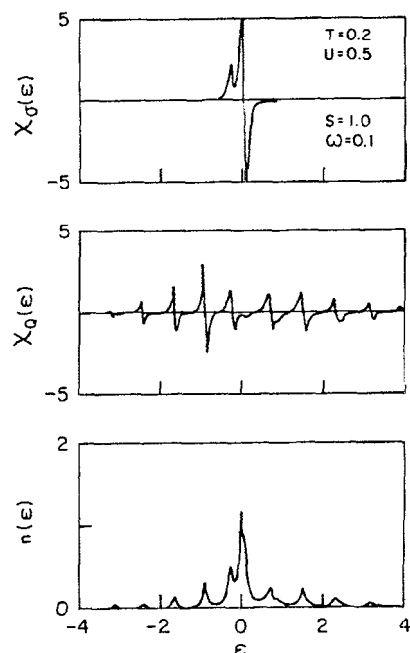


Figure 6: $n(\epsilon)$, $\chi_Q(\epsilon)$ and $\chi_\sigma(\epsilon)$, for the parameter set $T = 0.2$, $U = 0.5$, $S = 1.0$ and $w = 0.1$.

The “raw” results $n(\epsilon)$, $\chi_Q(\epsilon)$, $\chi_\sigma(\epsilon)$ in Figures 1-6 are a rather cumbersome picture of the results, if we need to extract from them the actual sequence of eigenvalue states and/or the actual weight of the several delta functions. The value 0.05 for the imaginary part of the energy seems to be adequate for a pictorial view, of course smaller values of δ will improve the accuracy but will generate also a scaling problem for the several weights, also increasing the computing time. If these “raw” results were needed then it is necessary to appeal to devices such as the analytic continuation algorithm mentioned above^[27]. We assert that the latter procedure is not needed beyond the calculation of the ground state, since as remarked above the Spin/Charge discriminator is a weak function of S . We notice too that a finite value of δ blurs out information, nevertheless by computing many observables this loss is partially retrieved, namely: in Figures 1 and 2, there are 4 eigenstates (see $n(\epsilon)$), from the susceptibilities; in Figure 1, eigenstates 2 and 3 are blurred into one state (they have the same parity), in Figure 2 eigenstates 3 and 4 are blurred into one state on the spin susceptibility, similarly eigenstates 1 and 2 on the charge susceptibility; so all three observables are needed to have a full view of the results, for our choice of δ . In Figure 4 the peak near the origin for $n(\epsilon)$ seems to be a single heavy weight state (a much smaller δ will show to be two eigenstates closely arranged), the spin susceptibility indicates this peak to be indeed two states with opposite parity and the charge susceptibility indicates these states to be clearly of the type STS. Therefore, if some information is lost due to the finite value of δ (but making the results both amenable to a pictorial

view and computationally fast), this loss is retrieved by computing other observables.

Finally in Figure 7 we present a Spin/Charge phase diagram for the diagonal case ($\kappa = 0$, see ref [28]). We plot the Spin/Charge interphase curve projected on the plane $T + U + S = 1$ (in suitable dimensionless units) for $w = 0.1$. The $C(S)$ label refer to the Charge (Spin) phase, the transition is smooth at the interphase. The interphase curve intersects the $U - S$ line at $U = 1/3, S = 2/3, T = 0$, as predicted from the small polaron transformation (see ref. [20] for exact results at $T = 0$). These results were obtained for $\delta = 0.001$, and remain insensitive as δ is decreased.

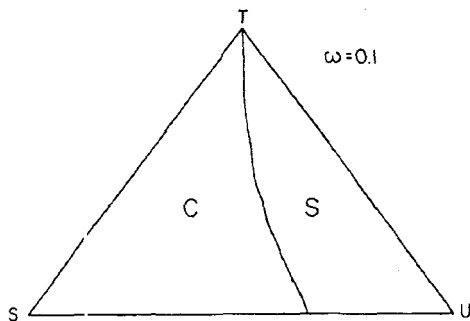


Figure 7: The Spin/Charge phase diagram projected on the plane $T + U + S = 1$ with $w = 0.1$.

V. Concluding Remarks

We presented a general method to solve Finite Peierls-Hubbard Systems and particularized to the diagonal phonon dimer. Our conclusions are summarized as follows:

i) our method proved to be advantageous over direct diagonalization^[23–26]. Our calculations involved 4×4 matrices and up to 30 continued fractions (in the probed region of parameter space). Direct diagonalization^[23–26] involves typical 300×300 matrices. To extend the latter method for the 3-site 3-electron 1-mode cluster (the smallest cluster to exhibit frustration and Jahn-Teller effects^[29], with the same degree of accuracy involves 2000×2000 matrices, for the 4-site 4-electron 1-mode cluster (solved in the adiabatic limit^[30]) will involve 7000×7000 matrices. Our method will deal at most with 20×20 and 70×70 matrices, respectively. If all lattice modes are to be included our method yields no increase in the matrices' dimensionality, but direct diagonalization will require 20000×20000 and 700000×700000 matrices, respectively. Thus, by increasing the cluster size to 4,6,8 sites, the matrices involved in our method are within manageable dimensions, not

so for the direct diagonalization method. Furthermore our method allows for the inclusion of more than one mode via a tested approximation^[12–14], and without any heavy increase of computational time. Beyond one mode, the direct diagonalization method becomes prohibitive.

- ii) our susceptibilities allow, at the cost of little extra computation, the study of the STS or QTS character of both the ground and the low lying excited states, related but not identical to the lattice deformation probed by direct diagonalization^[23–26]. In fact our bond strength parameter ξ (eq. (16)) plus our Spin/Charge discriminator ρ (eq.(15)) can completely probe both the STS/QTS character and lattice deformation for our system^[31]. Clearly a strong lattice deformation means a QTS and the converse is true for no deformation at all; nevertheless it is not clear for what intermediate lattice deformation value the system goes from a charge to a spin regime. Our method provides an unambiguous answer^[31].
- iii) our method when applied to clusters of increased size, will provide a systematic tool to probe the diverse approximations available for infinite systems, such as the adiabatic and mean field approximations.
- iv) the dimer case, is not a completely solved case, neither an uninteresting one (see for example^[29], where solely electronic correlations were considered), it stands as a particularly simple case displaying all full power the advantages of the method presented here.
- v) as for work in progress, we are probing the dimer with both diagonal and off-diagonal electron-lattice interactions for a full system characterization^[31].
- vi) as a final comment, we remark that our method might reminisce other methods hinging on continued fractions techniques, recurrence relations and the like (for example, Lanczos' Method, Mori's Approach, Haydock's Representation and so forth^[17]), nevertheless the present formalism should not be confused with the former ones, our's being substantially different and much more powerful, because even in the zeroth approximation (absence of phonon degrees of freedom) all fermionic correlations are accounted for.

Acknowledgments

This research work was partially supported by FAPESP (São Paulo, Brazil) Project number 91-2016-0.

References

1. S. Mazumdar and S. N. Dixit, *Pliys. Rev. Lett.* 51, 292 (1983).
2. S. Mazumdar, *Phys. Rev. B* 36, 7190 (1987).
3. F. C. Zhang and P. Prelovsek, *Pliys. Rev. B* 37, 1569 (1988).
4. S. Tang and J. E. Hirsch, *Pliys. Rev. B* 37, 9546 (1988).
5. I. I. Ukrainstii, *Sov. Phys. JETP* 49, 381 (1979).
6. J. Rossler and D. Gottlieb, *J. Pliys. Condens. Matter* 2, 3723 (1990).
7. K. Nasu and Y. Toyozawa, *J. Pliys. Soc. Jpn.* 51, 2098 (1982).
8. A. C. M. Stein-Barana, R. E. Lagos and G. A. Lara, *Proceedings VIII Simposio Chileno de Física, Valparaíso, Chile. Scientia LVII*, 485 (1992).
9. K. Král, *Czecl. J. Pliys. B* 26, 226, 660 (1976).
10. M. J. Rice, *Solid State Commun.* 31, 93 (1979).
11. R. E. Lagos and R. Friesner, *Phys. Rev. B* 29, 3045 (1984).
12. R. E. Lagos and R. Friesner, *J. Chem. Pliys.* 81, 5899 (1984).
13. R. E. Lagos and R. Friesner, *Chem. Pliys. Lett.* 122, 98 (1985).
14. Y. Won, R. E. Lagos and R. Friesner, *J. Chem. Phys.* 84, 6567 (1986).
15. R. Haydock, *Solid State Pliys.* 35, 215 (1980).
16. A. Sheuing, P. Reihcker, C. Durst and E. Sigmund, *Phys. Stat. Sol. (b)* 142, 179 (1987).
17. M. Cini and A. D'Andrea, *J. Pliys. C* 21, 193 (1988).
18. R. E. Lagos (in preparation).
19. S. Abe, *J. Phys. Soc. Jpn.* 59, 1496 (1990).
20. G. Mahan, *Many Particle Physics*, (Plenum, New York 1981).
21. Y. Toyozawa, *J. Pliys. Soc. Jpn.* 50, 1861 (1981).
22. S. Weber and H. Büttner, *Solid State Commun.* 56, 395 (1985).
23. W. Schmidt and M. Schreiber, *Z. Phys. B* 62, 423 (1986).
24. W. Schmidt and M. Schreiber, *J. Chem. Pliys* 86, 953 (1987).
25. C. R. Proetto and L.M. Falicov, *Pliys. Rev. B* 39, 7445 (1989).
26. Y. Inada and C. Ishii, *J. Pliys. Soc. Jpn.* 59, 612 (1990).
27. K. C. Hass, B. Velický and H. Ehrenreich, *Phys. Rev. B* 29, 3697 (1984).
28. S. Weinketz and R. E. Lagos, *Proceedings VIII Simposio Chileno de Física, Valparaíso, Chile. Scientia LVII*, 99 (1992).
29. M. Schreiber, *J. Pliys. Soc. Jpn.* 56, 1029 (1987).
30. J. Taltimoto and Y. Toyozawa, *J. Pliys. Soc. Jpn.* 52, 4331 (1983).
31. S. Weinketz and R. E. Lagos (in preparation).
32. R. E. Lagos, G. A. Lara and G. G. Cabrera, *Phys. Rev. B* (accepted 1993); *Proceedings VIII Simposio Chileno de Física, Valparaíso, Chile. Scientia LVII*, 405 (1992).